Stochastic gravitational-wave background on large cosmological scales

Rom, Tamara

University of Split
Faculty of Science

Stochastic gravitational-wave background on large cosmological scales

Master thesis

Tamara Rom

Split, July 2021

I wish to express my deepest gratitude to my mentor dr. sc. Zvonimir Vlah for supervising me and patiently giving me countless number of explanations on this topic. My sincere thanks to Assist. Prof. Dr. Marko Kovač for helping with administration we encountered. J., thank you for being my constant support.

Temeljna dokumentacijska kartica

Sveučilište u Splitu
Prirodoslovno – matematički fakultet
Odjel za fiziku
Ruđera Boškovića 33, 21000 Split, Hrvatska

Diplomski rad

Stohastička pozadina gravitacijskih valova na velikim kozmološkim skalama

Tamara Rom

Sveučilišni diplomski studij Fizika, smjer Astrofizika i fizika elementarnih čestica

Sažetak:

Svemir kakvog poznajemo, star je otprilike 13.7 milijardi godina, a prosječne je temperature od 2.73 K. Sastav današnjeg svemira čini otprilike 5% vidljive materije, 23% tamne materije i 68% energije u obliku kozmološke konstante ili nekog drugog oblika tamne energije. Postoje razni kozmološki modeli i modeli čestične fizike koji pokušavaju objasniti parametre koje mjerimo postojećim detektorima na Zemlji i u svemiru. Za opaženu strukturu smatra se da je posljedica malih početnih perturbacija koje je zatim inflacija, odnosno naglo širenje svemira, prenijela. Trenutna teorija bazira se na tome da se svemir širi i dalje, što se pripisuje tamnoj energiji. Uz barionsku i tamnu materiju te tamnu energiju, postoje još mnoge fizikalne opservable u svemiru, a jedna od njih su gravitacijski valovi. Gravitacijski valovi su pojam koji neizostavno vežemo uz kozmologiju, a čije je postojanje potvrđeno tek 2015. godine. Uz detektirane astrofizikalne gravitacijske valove, pretpostavljeno je postojanje primordijalnih gravitacijskih valova koji su nastali u razdoblju ranog svemira. U ovom radu, cilj je razviti mehanizam kojim ćemo, pomoću poznate teorije i podataka, moći razlikovati astrofizikalne od primordijalnih valova te time utvrditi njihovo do sada teoretizirano postojanje. Prvo uvodimo pregled standardnog kozmološkog Lambda-CDM modela, a zatim podjelu izvora gravitacijskih valova na astrofizikalne i promordijalne. Slijedi matematički formalizam za opis gravitacijskih valova. U poglavlju 3 uvodimo metodu pristranih (eng. *biased*) galaktičkih tragača koja se koristi u teoriji formiranja velikih struktura, a koju želimo primijeniti na gravitacijske valove. Uzimamo u obzir samo linearni dio perturbacijske teorije. Sama primjena je u sljedećem poglavlju te dobivamo spektar snage gravitacijskih valova u odnosu na spektar snage tamne materije. Na ovaj način, tretirajući gravitacijske valove kao skalare, dobijemo distribuciju tamne materije na velikim skalama. Simuliran je graf spektra snage materije, pomoću internetskog alata CAMB, a koristeći taj rezultat konstruiramo spektar snage gravitacijskih valova kao linearnog tragača pristranosti (eng. *bias*). Generiramo spektar za različite vrijednosti Hubbleove konstante i parametra pristranosti (eng. *bias*), pokazujući različitosti amplituda i ovisnosti o skali. Naši rezultati se stoga mogu koristiti kao komplementarne kozmološke probe u podacima za buduće svemirske detektore gravitacijskih valova poput LISA-e i drugih.

Ključne riječi: gravitacijski valovi, stohastička pozadina, tamna materija, pristranost, tragači, spektar snage

Rad sadrži: 28 stranica, 17 slika, 0 tablica, 26 literaturnih navoda. Izvornik je na engleskom jeziku.

Mentor: dr. sc. Zvonimir Vlah

Ocjenjivači: dr. sc. Zvonimir Vlah,
doc. dr. sc. Marko Kovač,
prof. dr. sc. Nikola Godinović

Rad prihvaćen: 5. 7. 2021.

Rad je pohranjen u Knjižnici Prirodoslovno – matematičkog fakulteta, Sveučilišta u Splitu.

Basic documentation card

University of Split
Faculty of Science
Department of Physics
Ruđera Boškovića 33, 21000 Split, Croatia

Master thesis

Stochastic gravitational-wave background on large cosmological scales

Tamara Rom

University graduate study programme Physics, orientation Astrophysics and Elementary Particle Physics

Abstract:

The Universe contains approximately 5% od visible matter, 23% of dark matter and 68% of energy in a form of cosmological constant or some other form of dark energy. Amongst these ingredients there are many other physical observables such as gravitatonal waves. While astrophysical gravitational waves were detected in 2015, primordial gravitational waves, generated in many theoretical models of the early universe, still await observational confirmation. Our goal is to formulate a method that is capable of distinguishing astrophysical from primordial wave signals. To achieve this, we use the biased tracer formalism, valid on large cosmological scales. Using the online tool CAMB, we produce the matter power spectrum and, using this result, construct the gravitational-wave power spectra as a linear biased tracer. We generate spectra for different Hubble constant and bias parameter values, showing the difference in the amplitude and scale dependence of the spectra. Our results thus show how gravitational-wave background signals can be used as complementary cosmological probes in the data from future gravitational-wave space detectors like LISA and others.

Keywords: gravitational waves, stochastic background, dark matter, bias, tracers, power spectrum

Thesis consists of: 28 pages, 17 figures, 0 tables, 26 references. Original language: English.

Supervisor: Dr. Zvonimir Vlah

Reviewers: Dr. Zvonimir Vlah,
Assist. Prof. Dr. Marko Kovač,
Prof. Dr. Nikola Godinović

Thesis accepted: July 5, 2021

Thesis is deposited in the library of the Faculty of Science, University of Split.

Contents

1 Introduction

It could be said that today's hottest topics in the society, especially amongst non-physicists, are related to the studies of the Universe and elementary particles. Those two hardly exclude each other once you study them - we could imagine the Universe as a soup of baryonic matter and some other unknown ingredients such as dark matter and dark energy. To be precise, our current knowledge of this cosmic soup says that there is around 5% of visible matter, 23% of dark matter and 68% of energy in a form of a cosmological constant or some other dark energy as shown in Figure 1 [1, 2]. Our Universe started in a Big Bang and is approximately 13.7 billion years old, while currently being at a temperature of around 2.73 K.The success of the Big Bang paradigm rests on a number of observational pillars: the Hubble diagram that measures expansion; light element abundances that are in accord with Big Bang Nucleosynthesis; temperature and polarization anisotropies in the cosmic microwave background that agree well with theory; and multiple probes of large-scale structure that also agree with models. However, this success has come at a price, we were forced to introduce several ingredients, as mentioned, that go beyond the Standard Model of particle physics; dark matter and dark energy which dominate the energy budget of the universe; and a mechanism generating the small initial perturbations out of which structure formed, the most popular explanation being inflation. [1]
These ingredients are shown as illustrations at Figure 1 and Figure 2.

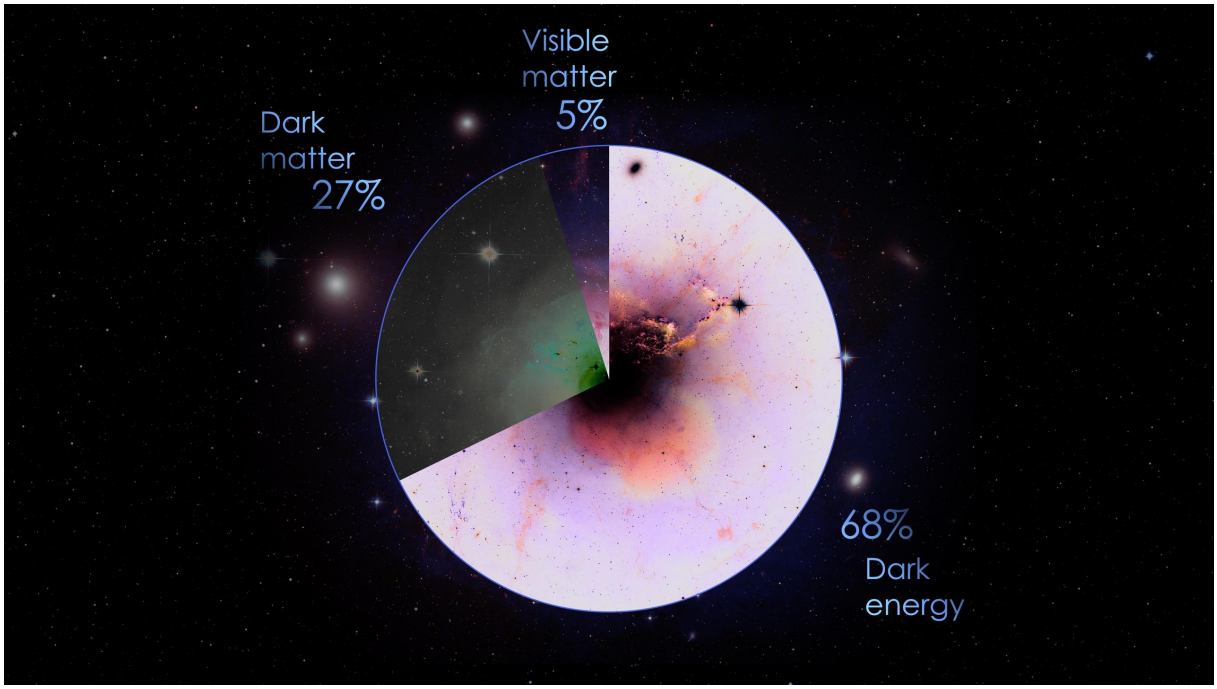

Figure 1: *A pie chart of what currently comprises our Universe. (Figure taken from [2])*

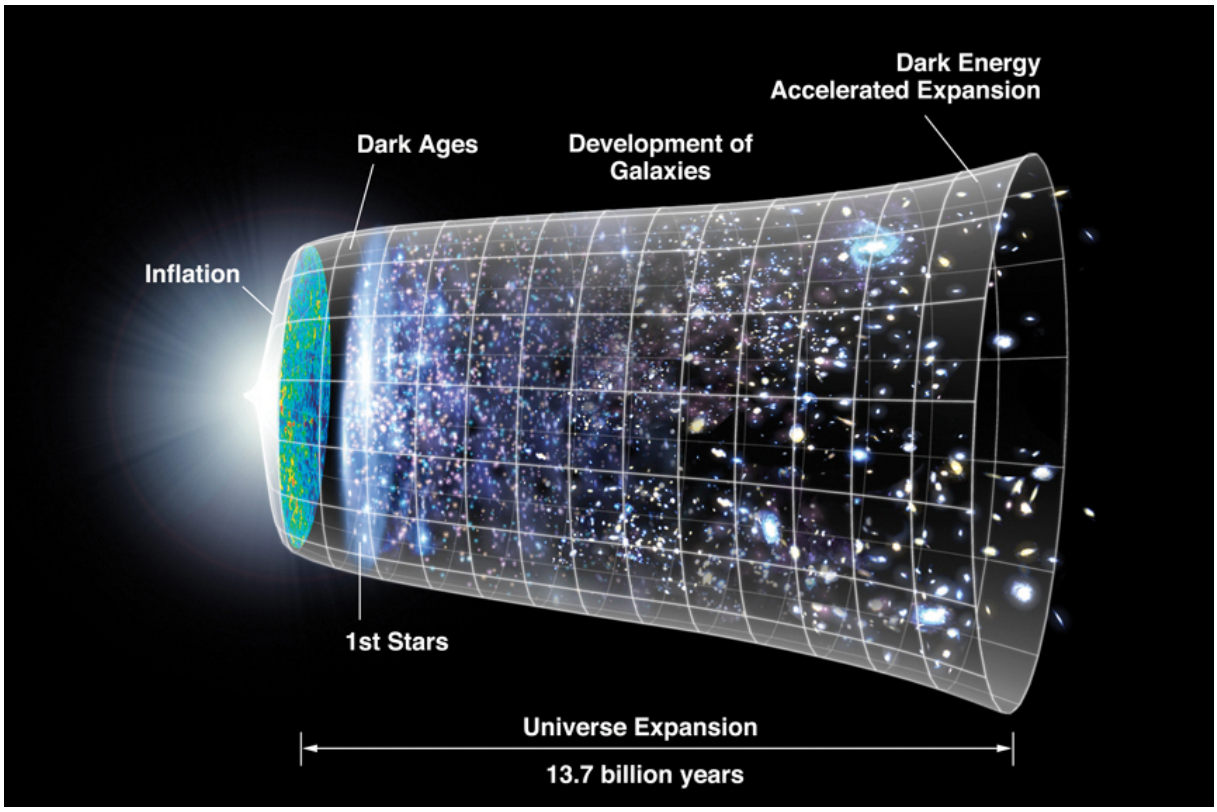

Figure 2: *The evolution of our Universe. (Figure taken from [3])*

1.1 A history of the Universe in a nutshell

We have solid evidence that the universe is expanding - this means that early in its history, the distance between us and distant galaxies was smaller than it is today. We conveniently introduce this effect by using a *scale factor* a, whose present value is set to 1 by convention, while at earlier times, a was smaller than it is today. We can imagine placing a grid in space which expands uniformly as time evolves. Points on the grid, which correspond to observers at rest, maintain their coordinates, so the *comoving distance* between two points - which just measures the difference between coordinates, and can be obtained by counting grid cells - remains constant. However, the physical distance is proportional to the scale factor, and the physical distances evolves with time. Directly related effect is that the physical wavelength of light emitted from a distant object is streched out proportionally to the scale factor, so that the observed wavelength is larger than the one at which the light was emitted. Conveniently, this stretching factor is defined as the *redshift* z:

$$1 + z \equiv \frac{\lambda_{\rm obs}}{\lambda_{\rm emit}} = \frac{a_{\rm obs}}{a_{\rm emit}} = \frac{1}{a_{\rm emit}}. \tag{1.1}$$

Additionally, the smooth universe is characterized by one other parameter - its geometry. There are three possibilities: Euclidean or a "flat universe" (particles travel in a parallel), closed (particles' path converge), open (particles' path diverge). General relativity connects energy and

geometry. This means that the total energy density in the universe determines the geometry: if the density is higher than a critical value, $\rho_c \approx 10^{-29}\mathrm{gcm}^{-3}$, the universe is closed; if the density is lower, it is open; if the density is equal to critical then it is a Euclidean universe. No matter how this seems unlikely to happen, all observations indicate that the universe is Euclidean to within errors and inflation provides a natural explanation for this. To understand the history of the universe, evolution of the scale factor a with cosmic time t has to be determined. At the earlier stage of the evolution of the universe, $a \propto t^{1/2}$, while at later times the dependence switches to $a \propto t^{2/3}$. The variation of the scale factor is determined by the evolution of the energy density in the universe. At earlier times, radiation dominates, while later, nonrelativistic matter accounts for most of the energy density. To quantify the change in the scale factor and its relation to the energy, *Hubble rate* is introduced as $H(t) \equiv \frac{1}{a}\frac{da}{dt}$, which measures how rapidly the scale factor changes. With subscript 0, we denote the value of a quantity today, so $H_0 \equiv H(t_0)$ is known as *Hubble's constant*. General relativity predicts that the scale factor is determined by the *Friedmann equation*:

$$H^2(t) = \frac{8\pi G}{3}\left[\rho(t) + \frac{\rho_c - \rho(t_0)}{a^2(t)}\right], \tag{1.2}$$

where G is Newton's constant, $\rho(t)$ is the energy density in the universe as a function of time with $\rho(t_0)$ its value today; ρ_c critical density. To use the Friedmann equation, we must know how the energy density evolves with time but this is a complicated question because ρ in it is the sum of several different components, each of which scales differently with time. Consider first nonrelativistic matter, which means that the energy of a given constituent particle is essentially equal to its rest mass energy, which remains constant with time. The energy density of a collection of these particles is therefore equal to the rest mass energy times the number density. The densities were necessarily larger when the scale factor was smaller. Apart from matter, there is a sea of massless photon that permeates the universe, discovered in 1965. These photons have traveled freely since the universe was very young. Nowadays, their wavelengths lie in the microwave part of the spectrum so they comprise what is called the cosmic microwave background (CMB). For further details, see [1].

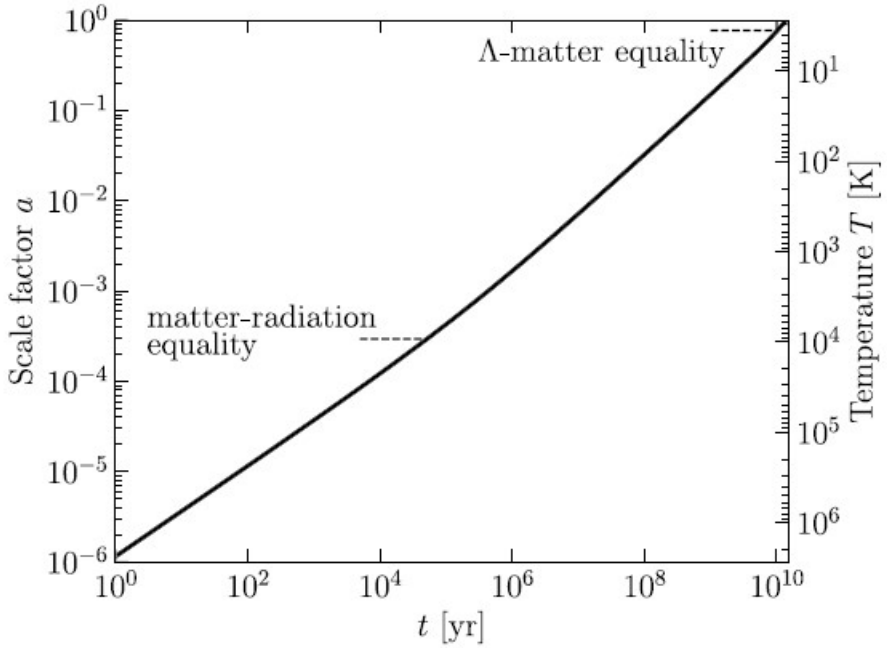

Figure 3: *Evolution of the scale factor of the universe with cosmic time. Today's universe corresponds to the upper-right corner of the plot, where $a(t_0) = 1$ and the temperature $T = 2.73$ K. In the very early universe, radiation was the dominant component and the scale factor increased at $t^{1/2}$. At the indicated point, the universe transitioned to matter domination, during which $a(t) \propto t^{2/3}$. Recently, the expansion law changed again due to dark energy, with $a(t)$ transitioning to an exponential function of time. [1] (Figure taken from [1])*

1.2 The topic of this thesis

In this thesis we build on these cosmological ingredients by introducing gravitational waves and the stochastic background that they produce. Gravitational waves have been of great interest in the last decade, especially since their first detection. It is expected that gravitational waves are going to be even more intensely studied in the following years. We could use gravitational waves as cosmological and astrophysical probes for our theories and that is where one of many of their interesting features lie. In this work, we would like to model their behaviour on large scales. In Chapter 2 we briefly introduce gravitational waves; their different sources; signal properties; and mathematical formalism behind them. This is followed by introducing bias galaxy tracers, in Chapter 3, that are often used in the theory of the large-scale structure. In Chapter 4 we apply bias to gravitational waves. Implications of this application and conclusions are drawn in Chapter 5.

2 Stochastic gravitational-wave background

2.1 Gravitational waves

Einstein's theory of General Relativity predicts many different phenomena such as black holes, gravitational lensing and gravitational waves (GW). Gravitational waves are the ripples in the fabric of spacetime and they contract or expand it on their way. There are various sources to gravitational waves, which will be discussed later in this chapter, but one way of producing them is in a binary system of two stars orbiting one another. Gravitational waves carry away angular momentum and energy from the forementioned system which can be indirectly detected. This has been done by R. Hulse and J. Taylor, while observing the pulsar PSR 1913+16 [4]. However, the first direct observation of gravitational waves was made in 2015 from a binary black hole merger, 100 years after the first theoretical prediction, by Laser Interferometer Gravitational-Wave Observatory (LIGO) and Virgo collaboration [5]. Figure 4 shows an illustration of the second detection of gravitational waves at LIGO.

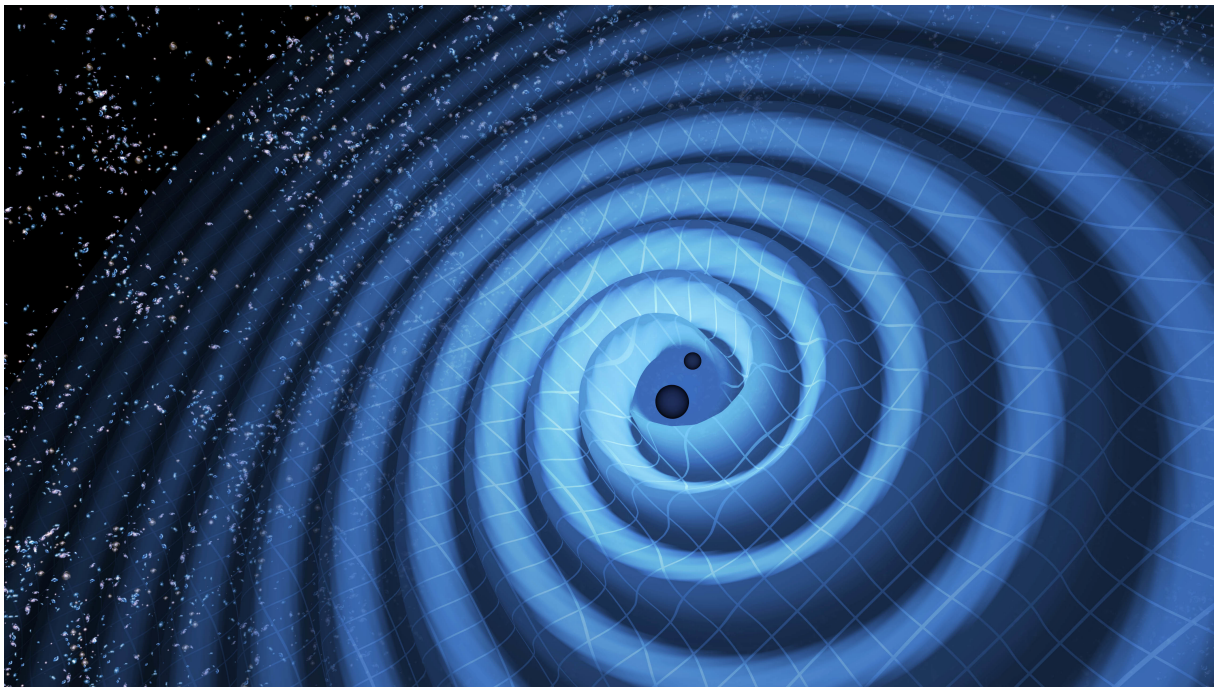

Figure 4: *This is an illustration of the second ever detection of gravitational waves at LIGO. It shows the merger of two black holes and the gravitational waves that ripple outward. The black holes were 14 and 8 times the mass of the Sun and, when they merged, formed a single black hole 21 times the mass of the Sun. If seen in reality, the area near the black holes would appear highly warped and the gravitational waves would be difficult to see directly. [6] (Figure taken from https://www.ligo.caltech.edu [6])*

2.2 Motivation

A stochastic background of gravitational radiation is a superposition of gravitational-wave signals that are either too numerous or too weak to individually detect. Such individual signals are thus unresolvable, unlike the large signal-to-noise ratio binary black hole (BBH) and binary neutron star (BNS) merger signals. Although, individual signals that contribute to the gravitational-wave background (GWB) cannot be resolved, the detection of such a background would provide useful information of statistical or population properties of the source. [7] The next step would be to create a GW analogue of the cosmic microwave background (CMB) shown in Figure 5, which is a sky map of the temperature fluctuations, relative to $T_0 = 2.73$ K isotropic component, in the CMB blackbody radiation [7, 9, 10]. The nature of the CMB is that it is a relic of the electromagnetic radiation, dating back to approximately 380,000 yr after the Big Bang [11]. At that time, the universe was at around 3000 K which is a low enough temperature to form first hydrogen atoms and, in the absence of free electrons, for photons to move unhindered [7]. What we see in the CMB is the "screenshot" of the density perturbations from the time of last scattering of photons, which is a "seed" for large-scale structure formation in the early universe [7]. Due to the different nature of gravitational interaction in comparison to the electromagnetic force, GWB would give information of the universe as it was about 10^{-22} seconds after the Big Bang [12]. This is why detecting cosmological GWB would be extremely important, since it would be our window into the earliest moments of the universe.

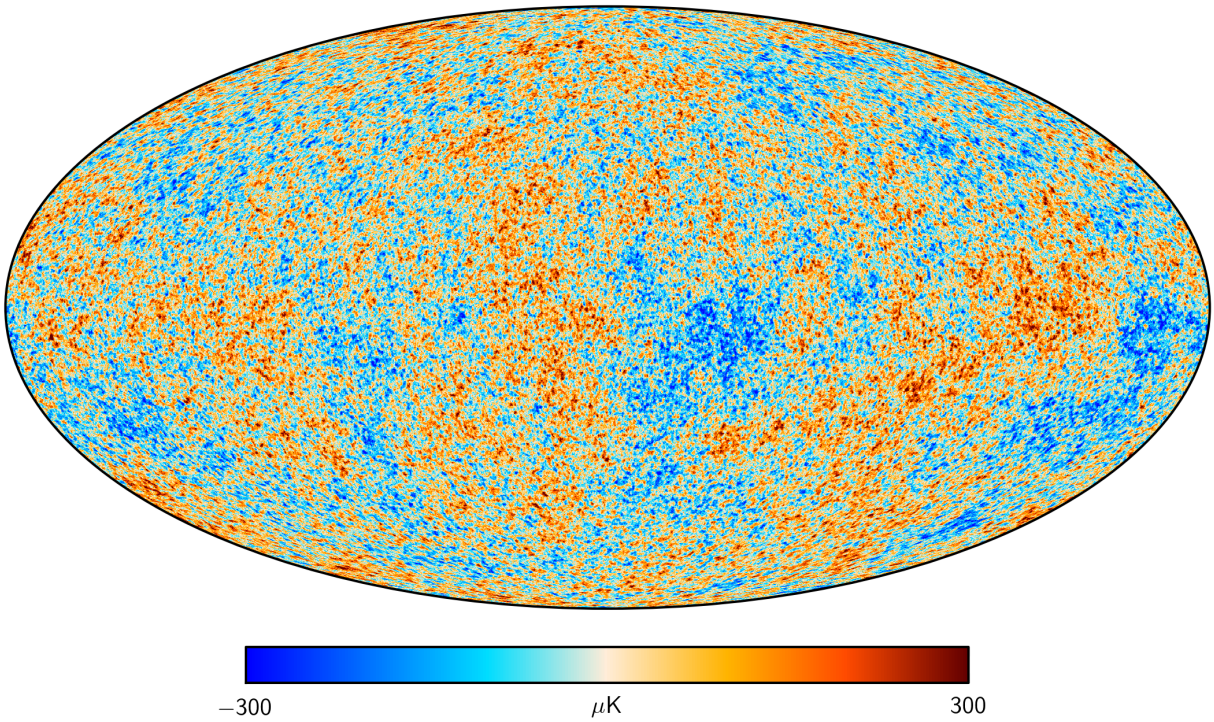

Figure 5: *Skymap of $\Delta T/T_0$ for the cosmic microwave background radiation [7]. (Figure taken from https://www.cosmos.esa.int [8])*

2.3 Different sources of gravitational-wave background

A stochastic background of gravitational radiation arises from an extremly large number of weak, independent and unresolved gravitational-wave sources [13]. Such backgrounds could have been produced in the early universe from inflation, phase transitions or cosmic strings [13]. Other way to produce a GWB is from many unresolved astrophysical sources, for example by combining signal from binary black hole and binary neutron star mergers that evolved from stars, the so called stellar-mass BBH and BNS mergers. Mass of the binary system is reciprocal to the frequency of the gravitational wave it produces. Since stellar-mass BHs and NSs have relatively small masses, the signal they produce is at the high frequency end (from around 10 Hz to a few kHz) of the spectrum. This part of the spectrum is in the sensitive band for the ground-based detectors like LIGO and Virgo. Systems that are bigger in mass produce lower-frequency GWs that are also expected to be a part of the gravitational-wave background and they are potentially detectable with proposed detectors such as space-based gravitational wave detector Laser Interferometer Space Antenna (LISA). If we were to plot a gravitational-wave spectrum, we obtain the Figure 6. Frequencies in Figure 6 range from 10^{-17} Hz, with a corresponding period equal to the age of the universe, to a few kHz, with a period of a few miliseconds. [7] Furthermore, the potential sources of gravitational-wave background are shown together with detectors relevant for the each frequency. Next, we will look deeper into the nature of the sources.

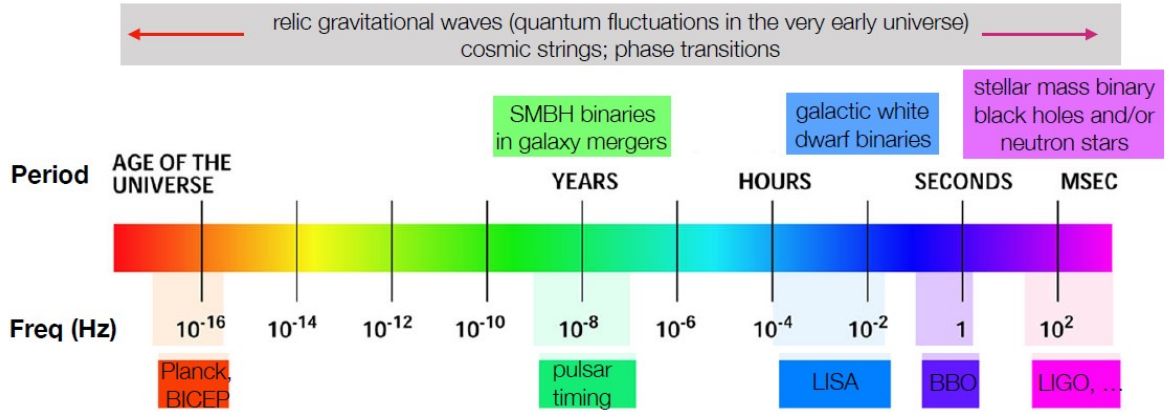

Figure 6: *Gravitational wave spectrum with detectors and potential sources of gravitational-wave background. GWB signal from cosmic strings and phase transitions depends on different parameters so they stretch across a whole spectrum and peak at basically any frequency. Relic gravitational waves, predicted by standard inflation, that constitute the primordial background, also stretch across the whole frequency band. [7] (Figure taken from [7])*

2.3.1 Cosmological or primordial sources

Gravitational-wave sources of cosmological origin are produced in the very early universe, before the formation of stars and galaxies. We could divide them into relic gravitational-waves due to inflation, those created by cosmic phase transitions and cosmic strings [13].

Relic GWs are quantum fluctuations in the geometry of spacetime, driven to macroscopic scales by inflation - a period of rapid expansion, mere 10^{-32} s after the Big Bang [7]. Cosmic phase transitions are macroscopic cosmic events so dramatic that they are capable of leaving imprint via non-adiabatic vacuum fluctuations and creation of particles, formation of defects, generation of magnetic field, generation of baryonic asymmetry, and the gravitational-wave background [14]. Cosmic strings are line-like topological defects associated with phase transitions in the early universe [7].

This relic background potentially has an effect on the polarization of the CMB radiation which makes it detectable [15].

2.3.2 Astrophysical sources

Compact astrophysical objects such as white dwarfs, neutron stars and black holes lay grounds to create gravitational waves. It is convenient to split astrophysical sources of gravitational waves into three main categories, according to the temporal behavior of the produced waveforms: burst, periodic and stochastic sources [13].

Burst sources can be divided into coalescing compact binaries and supernovae. Amongst all binary systems that radiate GWs, the most interesting ones of compact binaries are: neutron star - neutron star (NS/NS), neutron star - black hole (NS/BH) and black hole - black hole (BH/BH) binaries. [13] Compact binaries emit gravitational waves in three phases: (i) as they spiral in toward one another, (ii) as they merge to create a single object and (iii) as the resulting object rings down to a symmetric configuration, moreover, understanding each of these phases enhances our chances to detect the GW signals from binaries [16]. Neutron stars and black holes of stellar masses form in a gravitational core-collapse of a massive star, which leads to a supernova type II. The gravitational wave form produced in this type of event is unpredictable due to the yet incomplete knowledge of the collapse. [13]

Representative example for periodic gravitational waves are spinning neutron stars. Neutron star emits gravitational waves only if it has some kind of asymmetry because a rotating body that is perfectly symmetric around its rotationg axis does not emit GWs. There are several mechanisms that could cause the asymmetry. Stochastic sources are, like it's been previously mentioned, a large number of weak, independent, unresolved GW sources coming from the early universe or the populations of astrophysical sources (e.g. many binary systems). [13]

2.4 Signal properties

Different sources of GWB have different properties of the observed signal and these properties allow us to identify sources that contribute to the background. The difference is seen in terms of (i) angular distribution of GW power on the sky, (ii) temporal distribution and amplitude, (iii) power spectra. [7]

(i) Background that comes from cosmological sources such as cosmic strings or relic GWs is expected to be statistically isotropic, exactly like CMB. The GW power in this background is anisotropic since it follows the spatial distribution of its belonging sources, however, when averaged over different realizations of the sources, it has no preferred direction. Different statistically isotropic backgrounds are defined by different angular power spectra, C_l as a function of multipole moment l, where

$$C(\theta) = \sum_{l=0}^{\infty} \frac{2l+1}{4\pi} C_l P_l(\cos\theta), \tag{2.1}$$

is the angular correlation between GW power coming from two directions separated by angle θ. If the monopole, C_0, is the only non-zero element, it means that GWB is then exactly isotropic and that is the simplest model for stochastic backgrounds. On the other hand, there are statistically anisotropic backgrounds that have preferred directions in the distribution of power in the sky, even when averaged over different realizations of the sources. [7] Figure 7 shows a simulation of sky maps for statistically isotropic and anisotropic background.

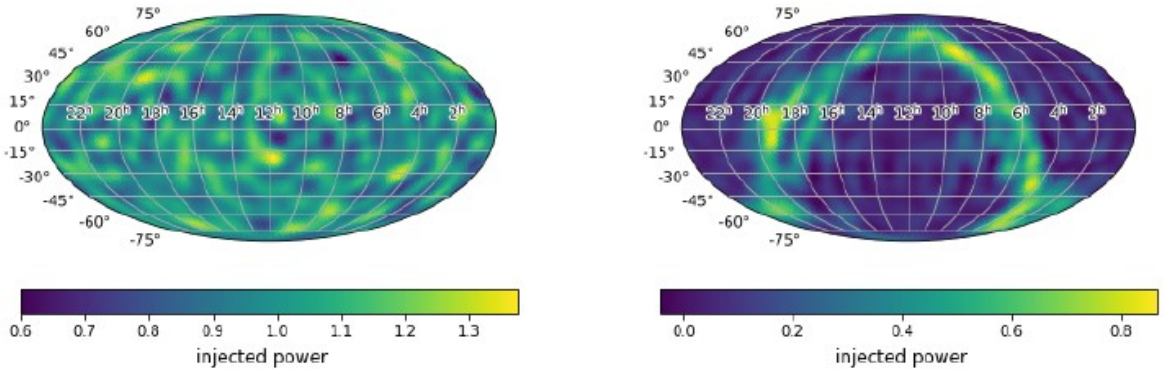

Figure 7: *Simulation of sky maps for a GW power of a statistically isotropic background (in the left panel) and an anisotropic background (in the right panel). The anisotropic background follows the galactic plane in equatorial coordinates as an example of one possible anisotropy. [7] (Figure taken from [7])*

(ii) Next difference in stochastic backgrounds is due to temporal distribution and amplitude. The rate estimates and durations of individual merger signals are such that the BBH background is expected to be popcorn-like which means that it is consisting of non-overlapping mergers, while that of BNS background is expected to be stationary and confusion-limited which means

that it is consisting of several overlapping BNS mergers at any instant of time. [7]

(iii) As shown in Figure 8, stochastic backgrounds can also differ in their power spectra. In the same figure, the simulated time-domain data, including the signals for an individual BNS merger and toy-model BBH ringdown (stage after the merging of two black holes, damping of the resulting black hole "ring" by emission of gravitational waves [17]), histograms and power spectra for three different types of gravitational-wave background. For these simulations, a sufficient number of individual BNS merger and BBH ringdown signals were overlapped to result in a Gaussian-stationary GWBs (shown in the second and the third columns). The difference between these backgrounds emerges in their power spectra which is in the fourth column. The power spectra for the BNS merger and BBH ringdown backgrounds are shaped the same way as those of an individual BNS merger or BBH ringdown, however, scaled by the total number of sources contributing to the background. [7]

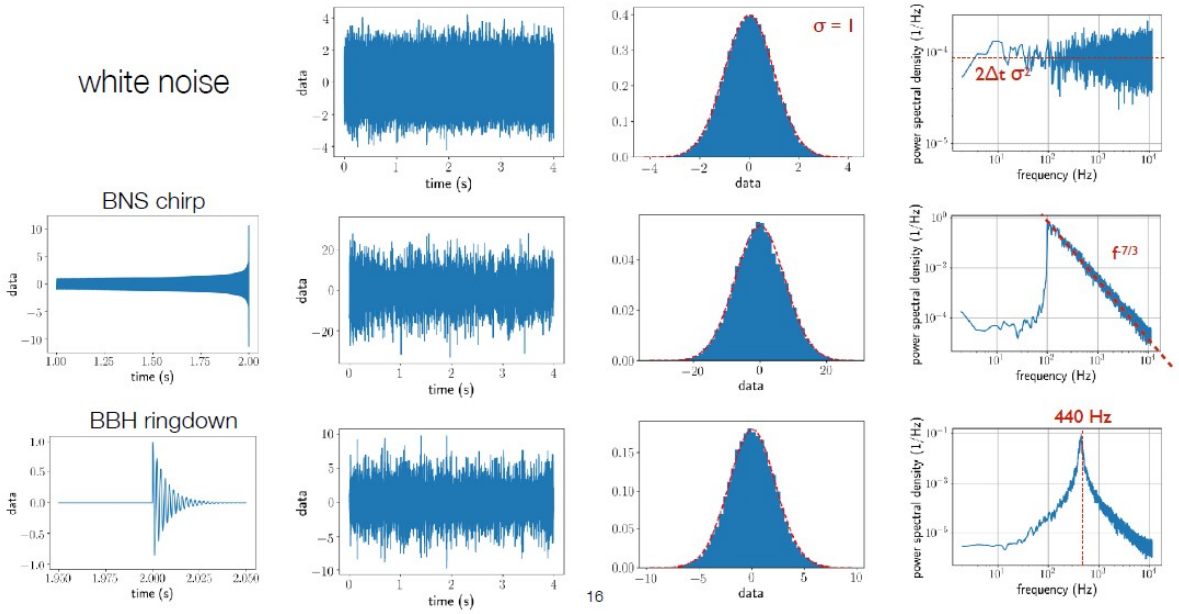

Figure 8: *Simulation of time-domain data, including the signals for an individual BNS merger and BBH ringdown, histograms and power spectra for three different types of Gaussian-stationary GWBs [7]. (Figure taken from [7])*

2.5 Mathematics of a stochastic background

We consider the combined signal for the background since the individual signals making a GWB are either too weak or too numerous to be individually detected. Another reason is that such signal is for all practical purposes random which is similar to the noise in a single detector. This means that we need to use ensemble averages of the metric perturbations to describe the GWB statistically. [7]

2.5.1 Plane-wave expansion of gravitational waves

Like previously mentioned, gravitational waves are time-varying perturbations to the geometry of space-time and they propagate from the source at the speed of light. The metric perturbations corresponding to a plane wave propagating in direction $\hat{k} \equiv -\hat{n}$, in transverse-traceless coordinates $(t, \vec{x}) \equiv (t, x^a)$ where $a = 1, 2, 3$, have two degrees of freedom. Those degrees of freedom correspond to the amplitudes of the plus $(+)$ and cross $(\times)$ polarizations of the gravitational wave (shown in Figure 9). [7]

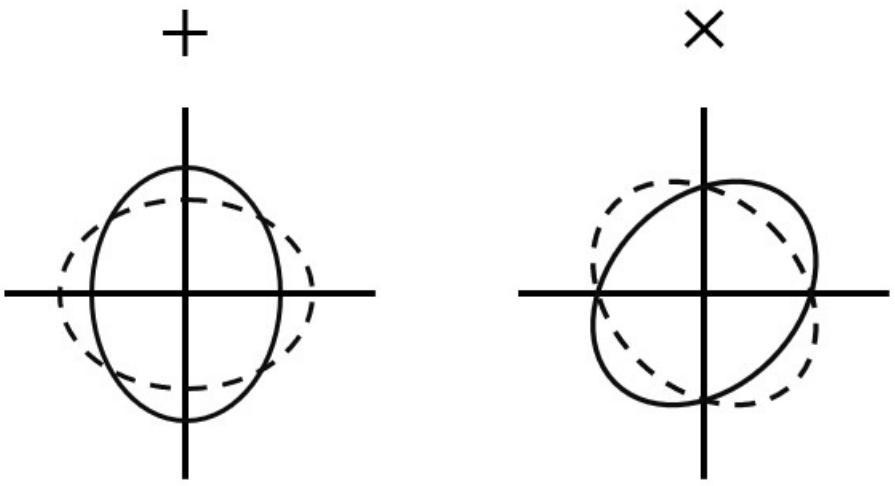

Figure 9: *Two possible orthogonal polarizations of a gravitational wave. Test particles, in a circular ring in the plane orthogonal to the direction of propagation of the wave, are deformed into ellipses as space is "squeezed" and "stretched" by the passing wave. [7]*

Taking everything mentioned into consideration, the metric perturbation for the most general GWB can then be written as a superposition of such waves

$$h_{ab}(t, \vec{x}) = \int_{-\infty}^{\infty} \mathrm{d}f \int \mathrm{d}^2\Omega_{\hat{k}} \sum_{A=+,\times} h_A(f, \hat{k}) e^A_{ab}(\hat{k}) e^{i2\pi f(t-\hat{k}\cdot\vec{x}/c)}, \tag{2.2}$$

where f denotes the frequency of the component waves, $\hat{k}$ direction of propagation and $A = +, \times$ their polarization. The direction to a particular GW source is given by $\hat{n} = -\hat{k}$ and the quantities $e^A_{ab}(\hat{k})$ are polarization tensors, given by

$$\begin{aligned} e^+_{ab}(\hat{k}) &= \hat{l}_a\hat{l}_b - \hat{m}_a\hat{m}_b, \\ e^\times_{ab}(\hat{k}) &= \hat{l}_a\hat{m}_b - \hat{m}_a\hat{l}_b, \end{aligned} \tag{2.3}$$

where $\hat{l}, \hat{m}$ are any two orthogonal unit vectors in the plane orthogonal to $\hat{k}$. For stochastic background analyses, $\hat{l}, \hat{m}$ are tipically taken to be proportional to the standard angular unit vectors tangent to the sphere in a way that $\{\hat{k}, \hat{l}, \hat{m}\}$ is a right-handed system (displayed in

Figure 10):

$$\begin{aligned}\hat{k} &= -\sin\theta\cos\phi\hat{x} - \sin\theta\sin\phi\hat{y} - \cos\theta\hat{z} = -\hat{r},\\ \hat{l} &= +\sin\phi\hat{x} - \cos\phi\hat{y} = -\hat{\phi},\\ \hat{m} &= -\cos\theta\cos\phi\hat{x} - \cos\theta\sin\phi\hat{y} + \sin\theta\hat{z} = -\hat{\theta}.\end{aligned} \tag{2.4}$$

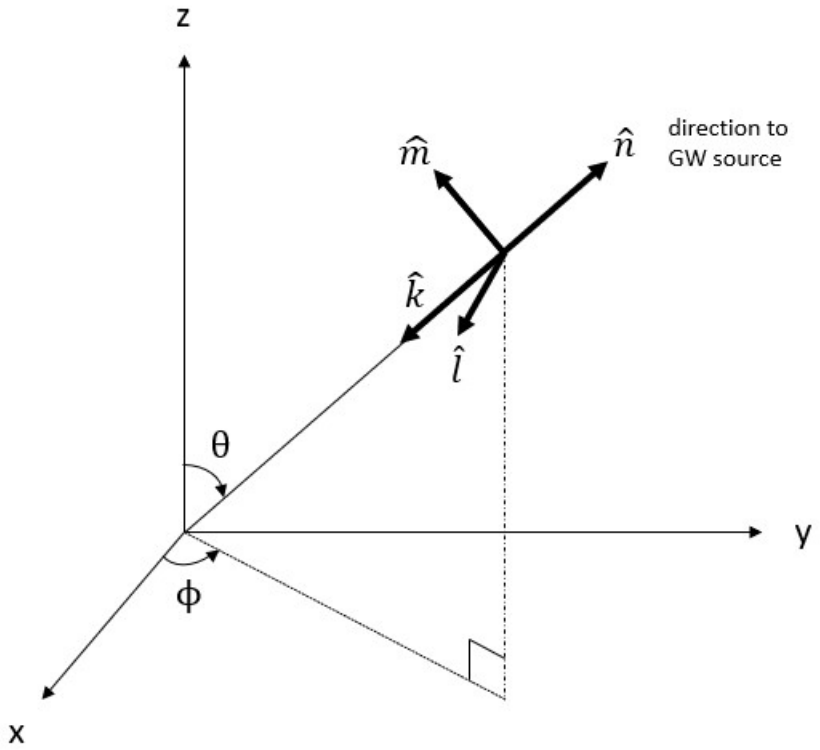

Figure 10: *Coordinate system and unit vectors we use in the plane-wave expansion of a gravitational-wave background [7].*

In the case of analyzing non-stochastic GW sources that have a symmetry axis, such as the angular momentum vector for binary inspiral, $\hat{l}$ and $\hat{m}$ are taken to be rotated relative to $-\hat{\phi}$ and $-\hat{\theta}$, where the rotation angle is the polarization angle of the source. [7]

2.5.2 Ensemble averages

The Fourier coefficients of the plane wave expansion are the quantitites $h_A(f, \hat{k})$ and since the metric perturbations for a stochastic background are random variables so too are the Fourier coefficients. This means that the probability distributions of the Fourier coefficients define the statistical properties of the background. We can assume that the expected value of the Fourier coefficients is zero, without losing the generality

$$\langle h_A(f, \hat{k})\rangle = 0, \tag{2.5}$$

where angle brackets mean ensemble average over different realizations (for example different backgrounds observed by different spatially-located observers in a homogeneous and isotropic universe) of the background. What's interesting are the second-order moments, or in other words, quadratic expectation values which denote possible correlations between the Fourier coefficients. If the background is unpolarized, stationary and isotropic, then we have

$$\langle h_A(f,\hat{k}) h^*_{A'}(f',\hat{k}')\rangle = \frac{1}{16\pi} S_h(f)\delta(f-f')\delta_{AA'}\delta^2(\hat{k},\hat{k}'), \tag{2.6}$$

where $S_h(f)$ is the strain power spectral density of the background, having units of strain^2 Hz^{-1}. Lets analyze the right-hand side of the Equation 2.6. Proportionality to the $\delta(f-f')$ is due to the assumption of stationarity which means that there is no preferrerd origin of time. Dependence on the polarization indices which are only via $\delta_{AA'}$ is due to the fact that the background is unpolarized, or in other words, the $+$ and $\times$ polarization components are statistically equivalent and uncorrelated with one another. Consequence of isotropy, or the fact that the power in the GWB has no preffered direction and that the GWs propagating in different directions have uncorrelated phases, is seen in the dependence on GW propagation directions via $\delta^2(\hat{k},\hat{k}')$. If we let the background to be either anisotropic or statistically isotropic, dropping the last assumption, the Equation 2.6 becomes

$$\langle h_A(f,\hat{k}) h^*_{A'}(f',\hat{k}')\rangle = \frac{1}{4} \mathscr{P}(f,\hat{k})\delta(f-f')\delta_{AA'}\delta^2(\hat{k},\hat{k}'), \tag{2.7}$$

where

$$S_h(f) = \int \mathrm{d}^2\Omega_{\hat{k}}\, \mathscr{P}(f,\hat{k}). \tag{2.8}$$

$\mathscr{P}(f,\hat{k})$ is the strain power spectral density per unit solid angle with units strain^2 Hz^{-1} sr^{-1}. For statistically isotropic backgrounds, the angular power spectrum is given by the coefficients C_l of a Legendre series expansion (Eq. 2.1) of the two-point function $C(\theta) \equiv \langle \mathscr{P}(f,\hat{k})\mathscr{P}(f,\hat{k}')\rangle_{skyavg}$, for all $\hat{k},\hat{k}'$ having cos$= \hat{k}\cdot\hat{k}'$. What's interesting is that for Gaussian backgrounds, all cubic and higher-order moments are either identically zero or can be written in terms of the second-order moments, thus, the quadratic expectation values of the Fourier coefficients give complete statistical properties of a Gaussian-distributed background. For more details, see [7].

2.5.3 Energy density spectrum

S_h, strain power spectral density of the GWB, can be related to the normalized energy density spectrum

$$\Omega_{\mathrm{gw}}(f) \equiv \frac{1}{\rho_{\mathrm{c}}}\frac{\mathrm{d}\rho_{\mathrm{gw}}}{\mathrm{dln}f} = \frac{f}{\rho_{\mathrm{c}}}\frac{\mathrm{d}\rho_{\mathrm{gw}}}{\mathrm{d}f}, \tag{2.9}$$

where the energy density in gravitational waves contained in the frequency interval f to $f+\mathrm{d}f$ is $\mathrm{d}\rho_{\mathrm{gw}}$ and the critical energy density that is needed to just close the universe today is

$\rho_c \equiv 3H_0^2c^2/8\pi G$. In case we use the relation which gives the energy density in gravitational waves in terms of the quadratic expectation values of the metric perturbations

$$\rho_{\rm gw} = \frac{c^2}{32\pi G}\langle \dot{h}_{ab}(t,\vec{x})\dot{h}^{ab}(t,\vec{x})\rangle, \tag{2.10}$$

we get this result

$$S_h(f) = \frac{3H_0^2}{2\pi^2}\frac{\Omega_{\rm gw}(f)}{f^3}. \tag{2.11}$$

Alongside $S_h(f)$ and $\Omega_{\rm gw}(f)$, we can describe the strength of a GWB with the dimensionless characteristic strain $h_c(f)$ which is defined as

$$h_c(f) = \sqrt{fS_h(f)}. \tag{2.12}$$

For backgrounds that are described by a power-law dependence on frequency,

$$h_c(f) = A_\alpha \left(\frac{f}{f_{\rm ref}}\right)^\alpha \quad \Leftrightarrow \quad \Omega_{\rm gw}(f) = \Omega_\beta \left(\frac{f}{f_{\rm ref}}\right)^\beta, \tag{2.13}$$

where α and β are spectral indicies and there is no sum over them. A_α is the amplitude of the characteristic strain and Ω_β is the amplitude of the energy density spectrum, both at some reference frequency $f = f_{\rm ref}$. Using these definitions and relationships between $\Omega_{\rm gw}(f), S_h(f), h_c(f)$, we obtain

$$\Omega_\beta = \frac{2\pi^2}{3H_0^2}f_{\rm ref}^2 A_\alpha^2, \quad \beta = 2\alpha + 2. \tag{2.14}$$

For standard inflatory backgrounds, we have $\Omega_{\rm gw}(f) = $ const., for which $\beta = 0$, and $\alpha = -1$, while for GWBs associated with compact binary inspirals, both neutron stars and stellar-mass black holes, and for supermassive black hole binaries we have $\Omega_{\rm gw} \propto f^{2/3}$ for which $\beta = 2/3$ and $\alpha = -2/3$ (relevant for advanced LIGO, Virgo, etc.). [7]
Characteristic strain dependence of frequency is shown in Figure 11 alongside different frequency bands where space and ground-based detectors operate.

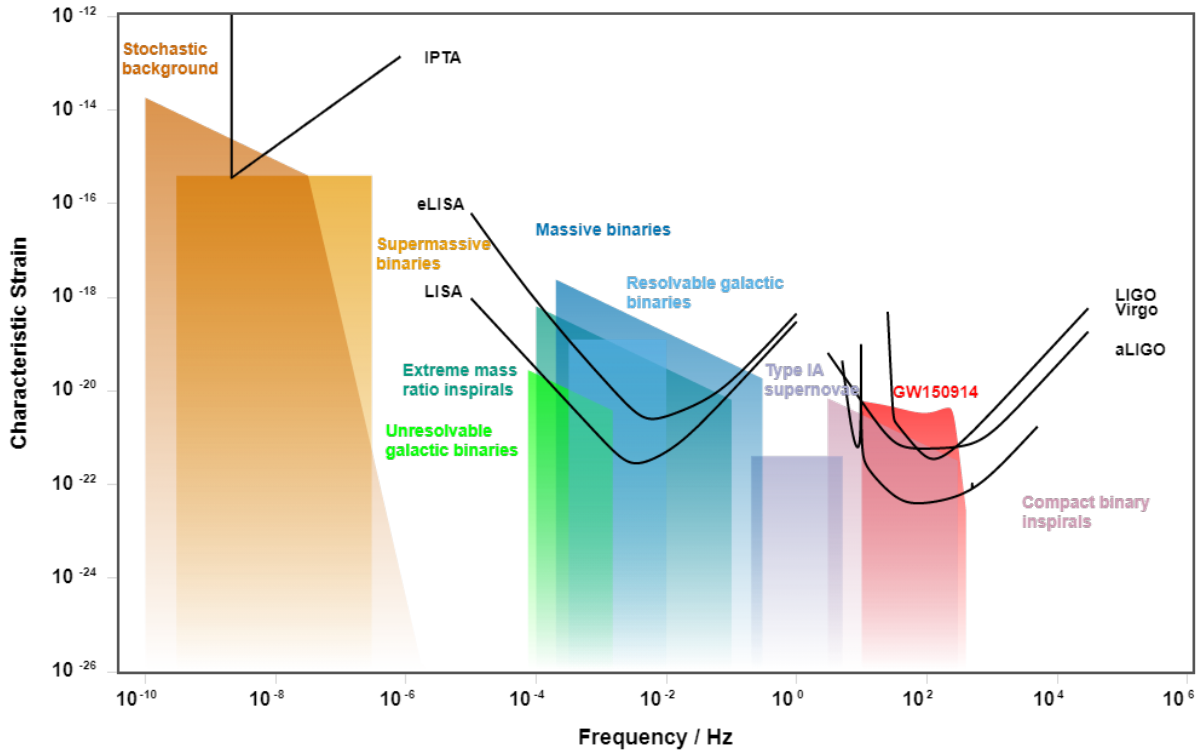

Figure 11: *Plot of the characteristic strain against the frequency of sources. Gravitational-wave spectrum, showing frequency bands where different detectors such as LISA and LIGO plan to operate or already operate, respectively. (Figure generated by http://gwplotter.com/, based on [18])*

3 Biased galaxy tracers

So far we have looked at gravitational waves and now we turn to biased tracers, let us see how they work.

There is no direct way of measuring the matter power spectrum; the bulk of matter is in form of dark matter and even much of the baryonic matter is not readily observable (e.g. dilute hot gas), however, there are many observables that probe the matter distribution indirectly [1].

Perhaps the most important observable is galaxy clustering which uses galaxies, or, generally speaking, any astrophysical object, as *tracers* of the large-scale matter distribution [1]. Such observed distribution of galaxies, quasars and clusters of galaxies - the large-scale structure (LSS) of the Universe (shown in Figure 12) is one of the foundations of our knowledge of the history of the Universe. If we understand how the distribution of tracers is related to the underlying distribution of matter, we can access a bunch of information on the composition of the Universe, properties of gravity, dark matter and dark energy, as well as the nature of producing the initial "seeds" of structure. [19]

We will make use of a relation known as *bias*, which connects luminous tracers (galaxies, voids, quasars, Lyman-α forest, 21cm hydrogen hyperfine structure transition lines, etc. [21, 22]) and matter, thus forming a key ingredient in the interpretation of the observed large-scale

structure. In standard cosmological models, the initial conditions of the LSS of the Universe is due to the quantum mechanical vacuum fluctuations and because of its origin, we cannot deterministically predict the precise initial conditions of the Universe as we observe it, therefore, our theoretical treatment of the LSS is based on describing random fields. [19]

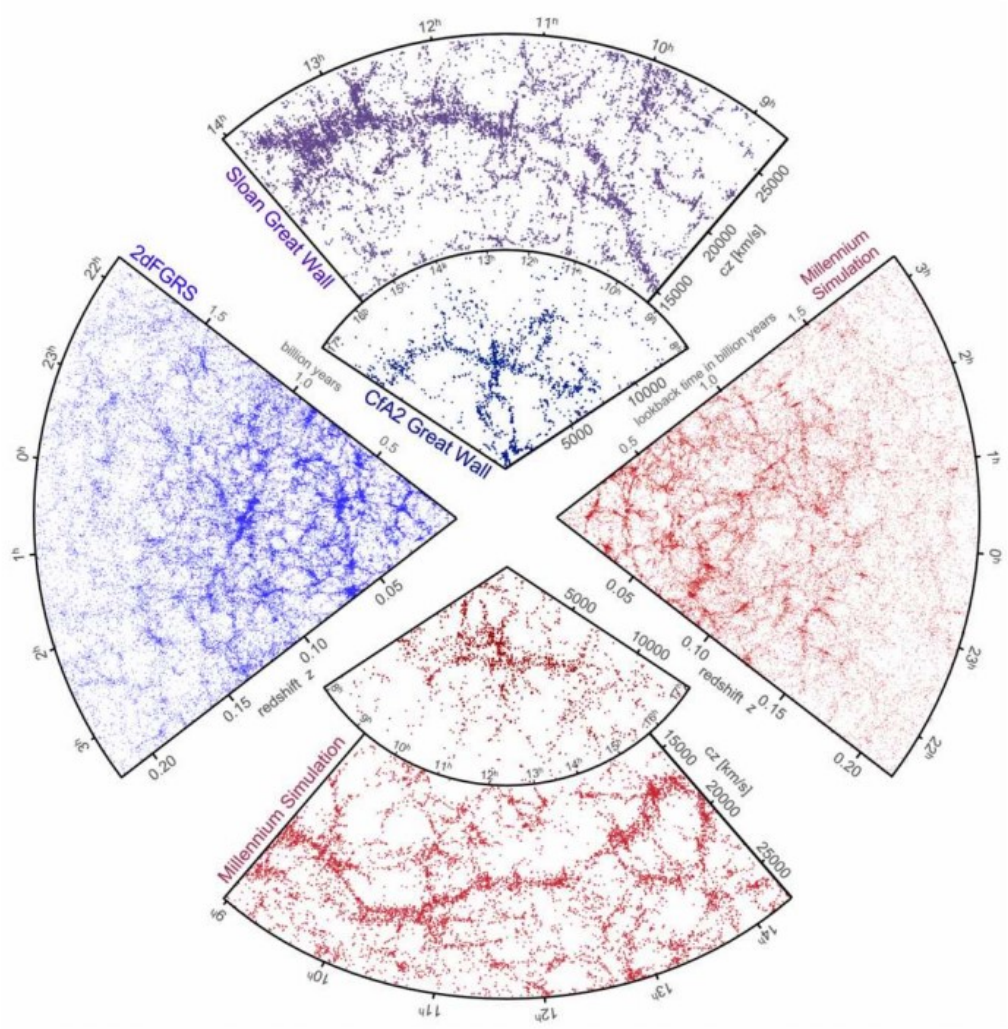

Figure 12: *2D slice projections of the locations of galaxies in CfA2, 2dF and SDSS galaxy redshift surveys are shown in the top left half. On the lower right, galaxies which were assigned to dark matter halos in the Millennium gravity-only N-body simulation using a semi-analytical prescription are shown - it is apparent that the simulation which assumes a flat ΛCDM cosmology, qualitatively reproduces the observed large-scale structure of the Universe quite well. [19] (Figure taken from [20])*

Beyond qualitative conclusion it is difficult to extract information from the 1-point function (mean of a random field) of galaxies - therefore, cosmological conclusions have been based on the next-order statistic of the galaxy density field, the two-point correlation function and its Fourier transform, the power spectrum [19]. Two-point correlation function basically tells us what is the probability that we will find two objects, lets says galaxies, within a fixed distance r of each other.

Consider a simple ansatz (linear bias relation) which locally relates the density contrast of galaxies or clusters of galaxies to that of matter at a fixed time

$$\delta_{\mathrm{g}}(\vec{x}) \equiv \frac{n_{\mathrm{g}}(\vec{x})}{\bar{n}_{\mathrm{g}}} - 1 = b_1 \delta_{\mathrm{m}}(\vec{x}) = b_1 \left(\frac{\rho_{\mathrm{m}}(\vec{x})}{\bar{\rho}_{\mathrm{m}}} - 1 \right), \tag{3.1}$$

where all the quantities are evaluated at the same fixed time, which is left implicit here, $\delta_{\mathrm{m}}(\vec{x})$ represents the matter overdensity, $\bar{n}_{\mathrm{g}}$ is the mean comoving number density of galaxies, while $\bar{\rho}_{\mathrm{m}}$ is the comoving background matter density and b_1 is a parameter called *bias* [19]. Because galaxies are complicated and highly nonlinear tracers of the LSS, their density perturbation is not the same as that of matter, however, their linear relation is a guranteed result at linear order in perturbations and on large scales [1]. In this thesis we will focus on linear theory and relation. We can write the Equation 3.1 as:

$$\delta_{\mathrm{g}}(\vec{x}) = b_1 \delta_{\mathrm{m}}(\vec{x}). \tag{3.2}$$

Bias parameter, b_1, incorporates the local physics (physics of small scales) such as galaxy mass, AGN feedback, metallicity, etc. While bias parameter completely describes all the complexities of galaxy formation, this is a nontrivial result that heavily relies on the fact that, on large scales, gravity drives the structure formation. Most of matter in the Universe comes in form of dark matter and this is the key information we use when connecting galaxies to matter like in Equation 3.2 because galaxies "float" in dark matter halos.

The Equation 3.1 of the simple linear bias can be generalized as

$$\delta_{\mathrm{g}}(\vec{x}, \tau) = \sum_{O} b_O(\tau) O(\vec{x}, \tau), \tag{3.3}$$

where O are operators, or statistical fields, that describe the galaxies' density dependance on their environment. Furthermore, each operator is multiplied by a corresponding bias parameter b_O which is a number at a fixed time and they are known as local bias parameters. Thus, we say that Eq. 3.3 can describe local density distribution. Equation 3.1 is an example of the Equation 3.3 with $O = \delta_{\mathrm{m}}$ and $b_O = b_1$. [19]

Overdensities are useful because we can obtain the correlation function whose Fourier transform is the power spectrum. The correlation function will only depend on the absolute distance from the objects due to the homogeneity and isotropy of our Universe. The power spectrum is then possible to observe using different detectors and sky surveys such as Planck or SDSS.

The correlation function, ξ, is mathematically defined as

$$\xi(|\vec{r}|) = \langle \delta_{\rm g}(\vec{x}) \delta_{\rm g}(\vec{x}') \rangle = \frac{1}{V} \int d^3\vec{x} \delta_{\rm g}(\vec{x}) \delta_{\rm g}(\vec{x} - \vec{r}), \tag{3.4}$$

where $\vec{r} = \vec{x}' - \vec{x}$. The relationship to the power spectrum, $P(\vec{k})$, is then derived as:

$$\xi(|\vec{r}|) = \int \frac{d^3k}{(2\pi)^3} P(k) e^{i\vec{k}\cdot(\vec{x}-\vec{x}')}. \tag{3.5}$$

The matter power spectrum, the Fourier transform of the correlation function, describes the difference between the local density and the mean density (so called density contrast) of the Universe as a function of scale. The overall shape of the matter power spectrum is best understood in terms of the linear perturbation theory analysis of the growth of structure, which predicts to first order how the power spectrum grows, but this will be further discussed in the next chapter. On large scales, gravity competes with cosmic expansion, and there is growth of structure in accordance with the linear theory. In this regime, the power spectrum is sufficient to completely describe the density field. [23] The spectrum as inferred from various cosmological probes is shown in Figure 13.

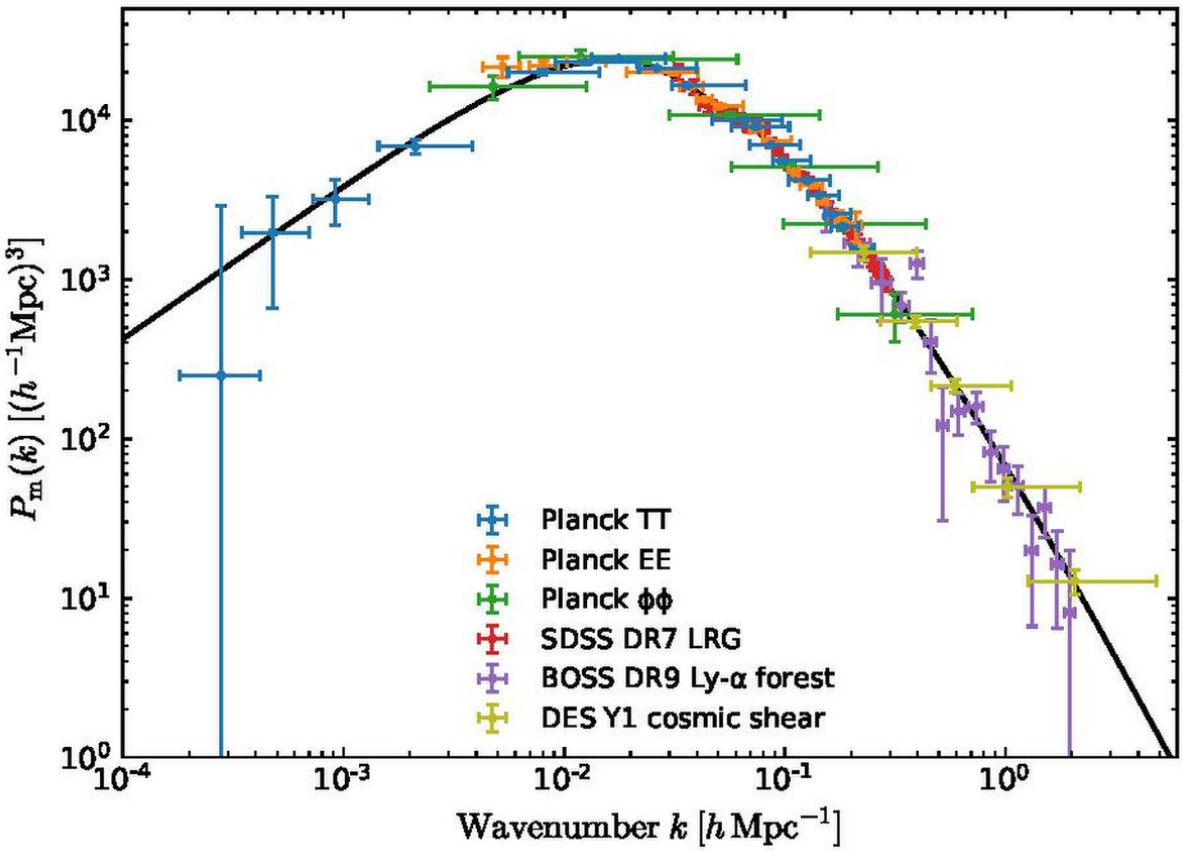

Figure 13: *Matter power spectrum inferred from various cosmological probes [23]. (Figure taken from [24])*

4 Method of bias applied to gravitational waves

For this description of bias applied to gravitational waves we can take as an example the sources that come from black holes. Black holes are mostly located in galaxies and we know that gravitational waves come from black hole mergers. Since they are connected to the galaxies, we can apply the idea, of bias for galaxies and matter, to gravitational waves and galaxies as well. What we get is

$$\delta_{\mathrm{GW}}(\vec{x}) = b_{\mathrm{GW}}\delta_{\mathrm{g}}(\vec{x}) = b_{\mathrm{GW}}b_1\delta_{\mathrm{m}}(\vec{x}) = c_1\delta_{\mathrm{m}}(\vec{x}), \tag{4.1}$$

where b_{GW} gives information, for example, on type of galaxy or gravitational wave source, other factors are same as in previous chapter and c_1 is the combined bias parameter, containing both information from matter and gravitational wave sources. However, to get the gravitational-wave overdensity here, we used the connection to the astrophysical sources. The motivation behind this is that we know astrophysical sources very well and if we derive an observable that gives us the whole overdensity, then we will be able to see if there is any discrepancy between the theory and the data. If there were any discrepancies and our theory for the astrophysical data has already been checked, that would mean we have successfully detected primordial gravitational waves. We are interested in is the correlation fuction of these overdensities

$$\xi_{\mathrm{GW}}(|\vec{r}|) = \langle \delta_{\mathrm{GW}}(\vec{x})\delta_{\mathrm{GW}}(\vec{x}')\rangle\,, \tag{4.2}$$

where $\vec{r} = \vec{x}' - \vec{x}$, but first have to asses several things.

Correlation function for galaxies in the previous chapter is for the 3D distribution, however, gravitational waves were defined over 2D spherical distribution. We want to derive the 3D gravitational-wave density field and "reduce" it to the 2D projection on the sky because the relations for bias are used for the three-dimensions only. We follow the formalism shown for galaxies in [1]. Let's define the distribution of distances, $W(\chi)$

$$W(\chi) = \frac{1}{N_{\mathrm{GW}}}\frac{dN_{\mathrm{GW}}}{d\chi}, \tag{4.3}$$

where N_{GW} is the total number of gravitational waves, $W(\chi)$ is normalized to unity over the interval $\chi \in [0, \infty)$ and χ represents comoving distance. Practically, $W(\chi)$ drops to zero below some minimum and above some maximum distances - gravitational waves at large distances are too faint to be detected and there are not that many gravitational waves at low redshifts because the volume is small. Here we assume that $W(\chi)$ is determined because photometric redshifts are difficult to determine on their own. It's important to define the Hubble rate which measures

how rapidly the scale factor a changes:

$$H(t) \equiv \frac{1}{a}\frac{da}{dt}. \tag{4.4}$$

The total comoving distance, χ, that is traveled by light that began its journey from an object at time t when the scale factor was equal to a (or redshift $z = 1/a - 1$) is then

$$\chi(t) = \int_t^{t_0} \frac{dt'}{a(t')} = \int_{a(t)}^1 \frac{da'}{a'^2 H(a')} = \int_0^z \frac{dz'}{H(z')}, \tag{4.5}$$

where we have changed the integration over t' to a', which brings in the additional factor $\dot{a} = aH$ in the denominator, and then finally to z'. Now, we can imagine dividing the sky area into small pixels and counting the gravitational waves in each pixel, futhermore, subtracting and dividing by the mean, we obtain the projected overdensity $\Delta_{\text{GW}}(\hat{\vec{n}})$. This gives us a superposition of many slices of 3D gravitational-wave density field at different distances χ, weighted by the distance distribution, so we obtain

$$\Delta_{\text{GW}}(\hat{\vec{n}}) = \int_0^\infty d\chi W(\chi)\delta_{\text{GW,obs}}(\vec{x} = \hat{\vec{n}}\chi, \eta = \eta_0 - \chi), \tag{4.6}$$

where η is a variable we can call comoving horizon and even conformal time and is defined as:

$$\eta(t) \equiv \int_0^t \frac{dt'}{a(t')}. \tag{4.7}$$

We use Δ_{GW} to distinguish the projected gravitational-wave density from the three-dimensional one $\delta_{\text{GW,obs}}$. The projection involves the gravitational-wave density given at different times η and more distant gravitational waves are seen at an earlier time since they all travel at the speed of light. Now we can insert the Fourier transform of $\delta_{\text{GW,obs}}$ and use the expansion of the exponential to get

$$\begin{aligned}\Delta_{\text{GW}}(\hat{\vec{n}}) &= \int_0^\infty d\chi W(\chi) \int \frac{d^3k}{(2\pi)^3} e^{i\vec{k}\cdot\hat{\vec{n}}\chi}\delta_{\text{GW,obs}}(\vec{k}, \eta(\chi)) \\ &= 4\pi \int \frac{d^3k}{(2\pi)^3} \sum_{lm} i^l Y_{lm}(\hat{\vec{n}}) Y^*_{lm}(\hat{\vec{k}}) \int_0^\infty d\chi W(\chi) j_l(k\chi)\delta_{\text{GW,obs}}(\vec{k}, \eta(\chi)),\end{aligned} \tag{4.8}$$

where we have abbreviated $\eta(\chi) = \eta_0 - \chi$ and $\sum_{lm} \equiv \sum_{l=0}^\infty \sum_{m=-l}^l$. The right-hand side is an expansion of $\Delta_{\text{GW}}(\hat{\vec{n}})$ in spherical harmonics, which can be read off as the coefficients of $Y_{lm}(\hat{\vec{n}})$:

$$\Delta_{\text{GW},lm} = 4\pi i^l \int \frac{d^3k}{(2\pi)^3} Y^*_{lm}(\hat{\vec{k}}) \int_0^\infty d\chi W(\chi) j_l(k\chi)\delta_{\text{GW,obs}}(\vec{k}, \eta(\chi)). \tag{4.9}$$

The angular power spectrum of gravitational-wave counts on the sky is proportional to the

expectation value of $|\Delta_{\mathrm{GW},lm}|^2$, thus we have to evaluate

$$\begin{aligned}\left\langle \Delta_{\mathrm{GW},lm}\Delta^*_{\mathrm{GW},l'm'}\right\rangle = (4\pi)^2 i^{l-l'}\int\frac{d^3k}{(2\pi)^3}\int\frac{d^3k'}{(2\pi)^3}Y^*_{lm}(\hat{\vec{k}})Y_{l'm'}(\hat{\vec{k'}})\int_0^\infty d\chi W(\chi)j_l(k\chi)\\ \times\int_0^\infty d\chi' W(\chi')j_{l'}(k'\chi')\left\langle\delta_{\mathrm{GW,obs}}(\vec{k},\eta(\chi))\delta^*_{\mathrm{GW,obs}}(\vec{k'},\eta(\chi'))\right\rangle,\end{aligned} \tag{4.10}$$

where the brackets $\langle ...\rangle$ denote an ensemble average over all realizations of the density field [1]. The ensemble average over the two fields immediately sets $\vec{k'}=\vec{k}$, due to homogeneity, and we can use the orthonormality of spherical harmonics to obtain

$$\left\langle \Delta_{\mathrm{GW},lm}\Delta^*_{\mathrm{GW},l'm'}\right\rangle = \delta_{ll'}\delta_{mm'}C_{\mathrm{GW}}(l) \tag{4.11}$$

where the angular power spectrum is defined as

$$\begin{aligned}C_{\mathrm{GW}}(l) = \frac{2}{\pi}\int k^2dk\int_0^\infty d\chi W(\chi)j_l(k\chi)\int_0^\infty d\chi' W(\chi')j_l(k\chi')\\ \times P_{\mathrm{GW,obs}}(\vec{k},\eta(\chi),\eta(\chi')).\end{aligned} \tag{4.12}$$

We see that the angular power spectrum $C_{\mathrm{GW}}(l)$ of gravitational waves involves the unequal-time power spectrum of GWs because we are projecting along the lightcone. This unequal-time power spectrum is nonzero because the density perturbations remain in place as they grow. Equation 4.12 is the exact result for the angular power spectrum of gravitational-waves, given their 3D power spectrum $P_{\mathrm{GW,obs}}(\vec{k},\eta,\eta')$ (allowing for anisotropy) and the selection function $W(\chi)$. Now, we can make an assumption, to simplify the equations, that we are looking at the small scales. For this assumption, $l\gg 1$, the gravitational-wave pairs contributing to $C_{\mathrm{GW}}(l)$ subtend a small angle on the sky, roughly $\theta\sim 1/l$, so for the Equation 4.12 in this regime, we get for the integral over k

$$\frac{2}{\pi}\int k^2dkj_l(k\chi)j_l(k\chi')P_{\mathrm{GW,obs}}(\vec{k},\eta,\eta'). \tag{4.13}$$

If $P_{\mathrm{GW,obs}}(\vec{k})$ were independent of k, it can be pulled out of the integral and it would reduce to

$$\frac{2}{\pi}\int k^2dkj_l(k\chi)j_l(k\chi') = \frac{1}{\chi^2}\delta^{(1)}_{\mathrm{D}}(\chi-\chi'). \tag{4.14}$$

With this simplification, the Equation 4.12 reduces to a single integral over χ, but in reality $P_{\mathrm{GW,obs}}$ is not independent of k. For high l, the product of spherial Bessel functions is very sharply peaked at $k\chi\approx k\chi'\approx\sqrt{l(l+1)}\approx l+1/2$. While $P_{\mathrm{GW,obs}}(\vec{k})$ varies slowly over the narrow range Δk over which the Bessel functions are nonzero, $\Delta k\sim 1/(l\chi)$, we can

approximate it as constant. The described approximation is known as the Limber approximation and it is usually very accurate at $l \gtrsim 20$. This approximation is also very useful since many sky surveys are limited to a smaller angle on the sky and not the whole field. The core prediction of this approximation is

$$C_{\mathrm{GW}}(l) = \int \frac{d\chi}{\chi^2} W^2(\chi) P_{\mathrm{GW,obs}} \left(k = \frac{l+1/2}{\chi}, \mu_k = 0, \eta(\chi) \right), \tag{4.15}$$

which is easier to calculate than the Equation 4.12. In Limber aproximation $\chi = \chi'$ which implies $\eta(\chi') = \eta(\chi)$ so the Equation 4.15 only involves the equal-time power spectrum. It also means that the k modes involved do not have a line-of-sight component since that would mean different distances of different points along the perturbation, in other words $\chi' \neq \chi$, so, k has to be transverse to the line of sight: $\mu_k = 0$. [1]

Our goal was to get to the Equation 4.15 since it can give us an observable that is useful for detectors. However, we should discuss the gravitational wave power spectrum element in that equation. In the Equation 4.15, $P_{\mathrm{GW,obs}}$ is defined in our regime as

$$P_{\mathrm{GW,obs}}(\vec{k}, \eta, \eta') = c_1(\eta) c_1(\eta') P_{\mathrm{m}}(\vec{k}, \eta, \eta') \tag{4.16}$$

following from the Equation 4.2. Next, we can state P_{m} of dark matter explicitly as

$$P_{\mathrm{m}}(\vec{k}, \eta, \eta') = D_+(\eta) D_+(\eta') P_{\mathrm{m}}(\vec{k}, 0, 0), \tag{4.17}$$

where D_+ denotes the linear growth factor in the density and $P_{\mathrm{m}}(\vec{k}, 0, 0)$ is commonly referred to as the primordial matter power spectrum which is related to the physics of inflation [23]. The simplest primordial matter power spectrum is the Harrison Zel'dovich spectrum, which characterizes $P_{\mathrm{m}}(\vec{k})$ according to a power law, $P_{\mathrm{m}}(\vec{k}) = Ak$, where A represents the scalar spectral index or the amplitude of fluctuations in the spectrum [23]. It is worth noting that in the Harrison Zel'dovich spectrum, the power of k is not exactly equal to 1 but around 0.9. In Figure 14, the simulation of the matter power spectrum is shown for different values of the Hubble constant, H_0, that have been possible candidates for the true value of H_0. This simulation is made using online tool CAMB that has various cosmological parameters already given. Specifically here, we used that the cold dark matter is around 23% and baryonic around 5% so the total matter is around 28%.

What interests us more than the matter power spectrum, is the simulation of the gravitational wave power spectrum. For when the bias parameter equals to 1 it is the same as the matter power spectrum shown in Figure 14. However, for different values of the bias parameter we have a different picture. This difference is shown in Figure 15 for when the Hubble constant, H_0 is equal to 67 km s^{-1} Mpc^{-1}. This value is chosen because according to the latest Planck collaboration data that is close to the current value of H_0 [26]. Bias in the legend means that

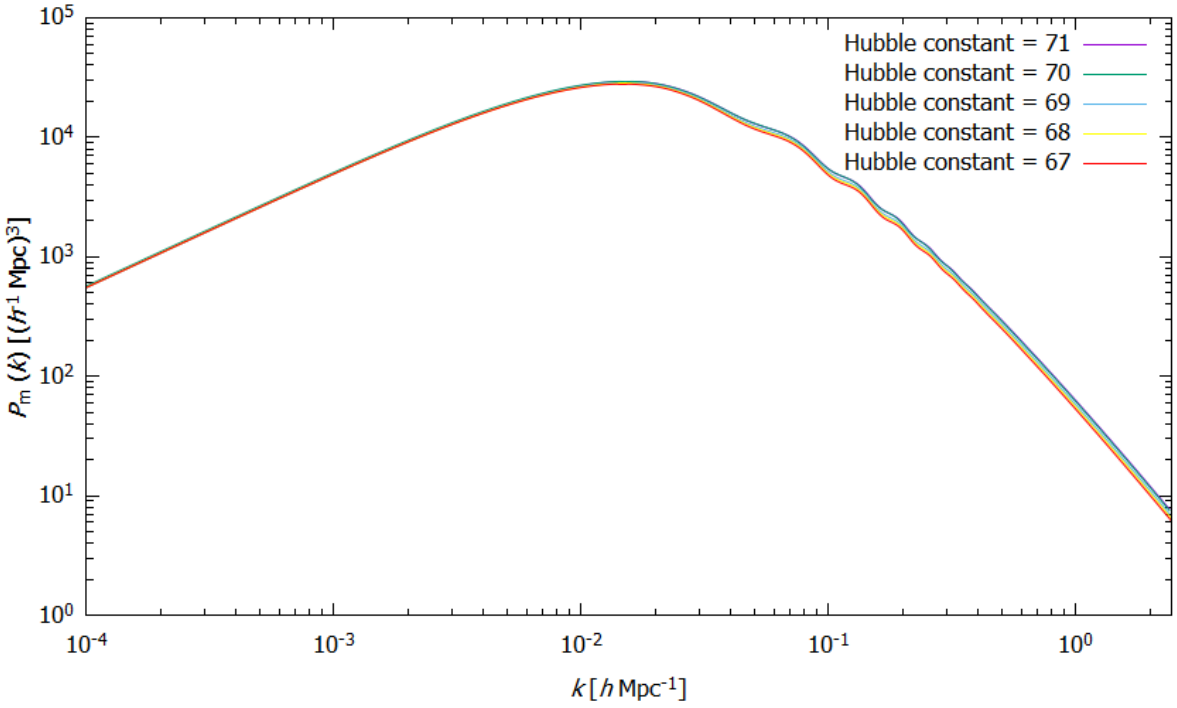

Figure 14: *Simulation of the matter power spectrum using online tool CAMB. This figure also represents the gravitational wave power spectrum for when bias parameter equals to 1 according to the Equation 4.16. URL given at [25].*

$c_1(\eta)c_1(\eta') = 1$, $c_1(\eta)c_1(\eta') = 2$, etc. The shape and the amplitude of this spectrum gives us astrophysical information, while we can only get cosmological from the dependence on the dimensionless number h which defines the Hubble constant as $H_0 = 100\,h\,\mathrm{kms}^{-1}\mathrm{Mpc}^{-1}$.

Figure 16 illustrates the physical reason behind the Limber approximation. Focusing on small scales corresponds to looking at small angles, $\theta \sim 1/l \ll 1$. Modes with longitudinal wavenumber $\mu_k k$ much greater than χ^{-1} do not give rise to angular correlations because of cancelations along the line of sight - only modes with $\mu_k k$ of order χ^{-1} or smaller lead to angular correlations. Thus, the relevant transverse wavenumbers l/χ are much larger than the relevant longitudinal wavenumbers and we can neglect the latter which then corresponds to setting $\chi' = \chi$. [1]

Finally, the angular correlation fuction $w_{\mathrm{GW}}(\theta)$ can be written. On small scales, in the flat-sky approximation, we can treat $C_{\mathrm{GW}}(l)$ as the 2D power spectrum on a plane, so

$$w_{\mathrm{GW}}(\theta) = \int \frac{d^2l}{(2\pi)^2} e^{i\vec{l}\cdot\vec{\theta}} C_{\mathrm{GW}}(l). \tag{4.18}$$

$C_{\mathrm{GW}}(l)$ depends only on the magnitude of l so the angular part of the integration over l is

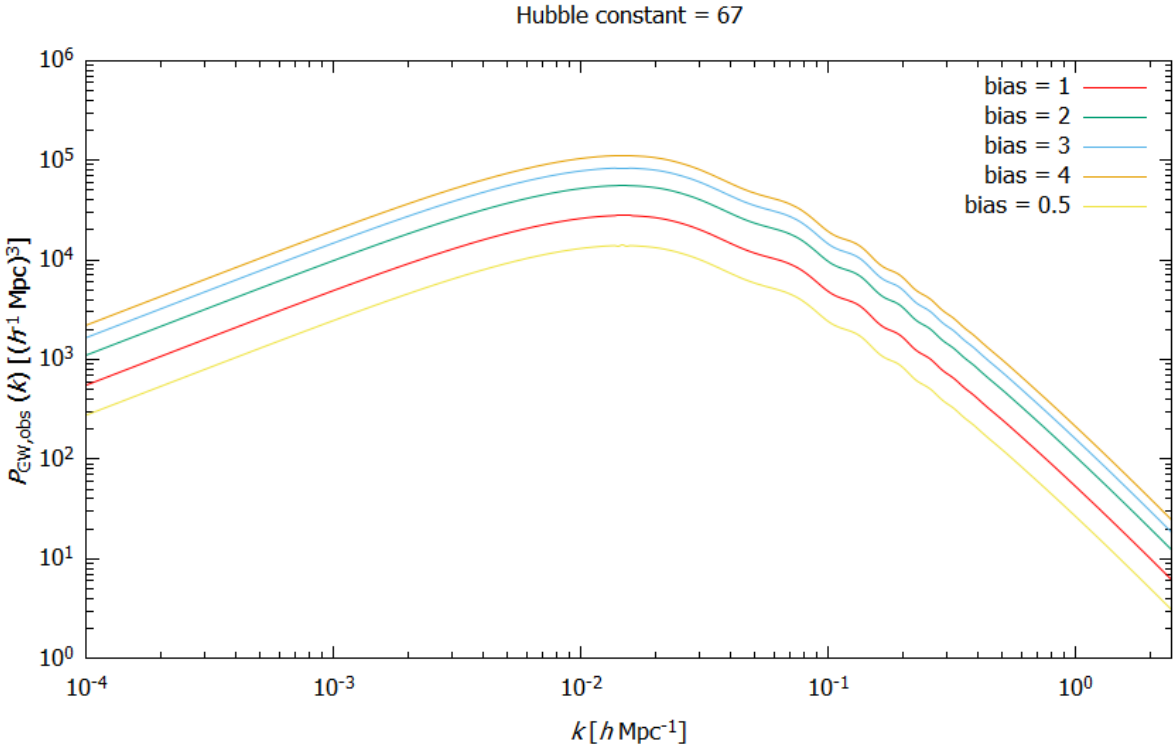

Figure 15: *The simulation of the gravitational wave power spectrum derived from the matter power spectrum by multiplying with different values of bias.*

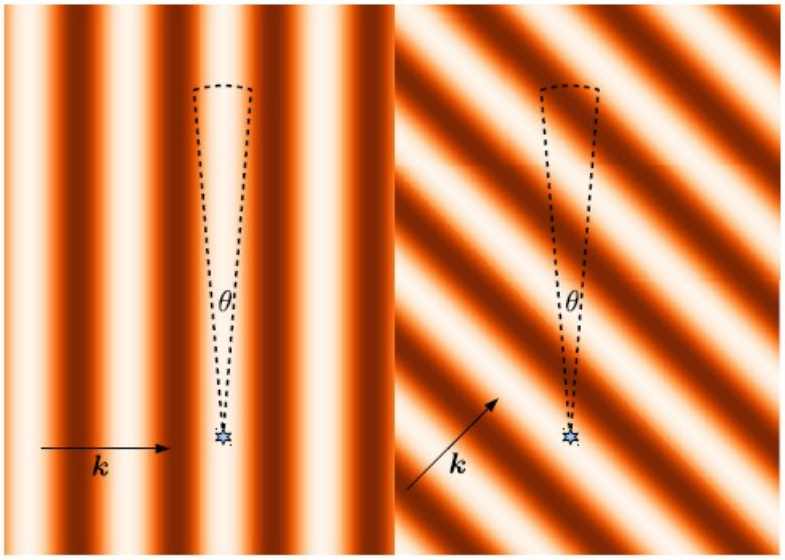

Figure 16: *Two plane-wave perturbations and their contributions to the angular power spectrum [1]. Left panel shows a transverse mode with $\mu_k k < \chi^{-1}$, while the right panel shows a perturbation with longitudinal wavenumber $\mu_k k \gg \chi^{-1}$ (the $\hat{\vec{z}}$ direction is vertical) [1]. Angular correlations due to the mode in the right panel are negligible since there are cancelations along the line of sight, while those do not occur for the transverse mode on the left [1]. (Figure taken from [1])*

$\int_0^{2\pi} d\Phi e^{il\theta\cos\Phi}$ which is proportional to $J_0(l\theta)$, the Bessel function of order zero. [1] Finally,

$$w_{\rm GW}(\theta) = \int_0^\infty \frac{dl}{2\pi} l C_{\rm GW}(l) J_0(l\theta). \tag{4.19}$$

Figure 17 shows the projected correlation function measured by the Dark Energy Survey (DES) for the galaxies. However, the same could be done by observing gravitational waves. This could then be used for many cosmological tests.

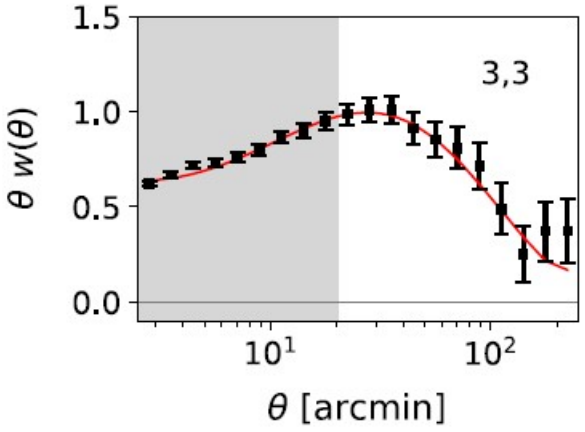

Figure 17: *Angular correlation function of galaxies in the photometric Dark Energy Survey. The correlation function $w(\theta) = w_{\rm g}(\theta)$ has been multiplied by θ in order to reduce the dynamic range, as $w_{\rm g}$ grows strongly toward small θ. The gray region involves comoving scales smaller than 8 h^{-1} Mpc, which are significantly affected by nonlinear evolution and bias. The line shows the best-fit model based on the linear bias. [1] (Figure taken from [1])*

5 Implications and conclusion

In this thesis we first review the standard cosmological model. Next we introduce the reader to the basic cosmological terms needed, followed by a mathematical formalism behind the gravitational waves and their features that are important for the ground-based detectors such as LIGO and Virgo, but also future space detectors such as LISA. The categorization of astrophysical and cosmological gravitational-wave sources is made according to their detected and proposed features. Furthermore, we describe the basics of bias galaxy tracers and the worth of using bias that is commonly used in the theory of the large-scale structure formation.

The novel and original content of the thesis is presented in Chapter 4. In this chapter we are applying the bias tracer method to the gravitational waves. This means that we use traces of dark matter to outline where our gravitational waves should be "clumped" together. Or vice versa, we are using gravitational waves as one of the tracers of dark matter fluctuations. We do this using bias formalism on variables such as matter power spectrum and angular power spectrum. Further work could be done by simulating the Equation 4.15 for the data we got from CAMB. The approach, describing the distribution of stochastic gravitational wave sources as being proportional to dark matter fluctuations, is a valid description on the largest cosmological scales.

Moreover, for the final procedure, we simplify the tensor nature of gravitational waves, and use the approach of modeling the gravitational waves source signals as scalar field. This procedure is justified since most detectors, that are used for detecting gravitational waves, still don't detect the polarization of the wave. Our approach can be readily modified in the future to incorporate the outlined tensor formalism.

Our results are useful for various gravitational-wave detectors for a given matter and gravitational-wave power spectrum, which are equivalent for the unity bias value. In general, bias values do not necessarily have to be equal to unity, different amplitudes of the spectrum are expected for different types of biased tracers. On the other hand the shape of the power spectrum, i.e. the dependence on the wave number, can differ for different values of cosmological parameters like the Hubble constant, as is shown in Figures 14 and 15. These results can be used to test current theories and data, such as inflation, Lambda-CDM model and gravity. For example, primordial waves have not yet been detected and are only speculated by the current cosmological theories of inflation. The power of applying the bias method to gravitational waves lies in the fact that once we measure the correlations of gravitational wave stochastic background, we can see if it matches the theoretical prediction obtained for astrophysical sources. Any unaccounted residual signal on large scales would indicate the potential primordial gravitational wave origin.

6 Bibliography

[1] Dodelson, S. and Schmidt, F., *Modern Cosmology Second Edition*, Academic Press, 2021

[2] NASA, Goddard Media Studios, URL: https://svs.gsfc.nasa.gov/12307 (25.06.2021.)

[3] NASA, Roman Space Telescope, Gallery, URL: https://roman.gsfc.nasa.gov/gallery-scientific_images.html#images-6 (25.06.2021.)

[4] Hulse, R. A. and Taylor, J. H., *Discovery of a pulsar in a binary system*, Astrophysical Journal, vol. 195, Jan. 15, 1975, pt. 2, p. L51-L53

[5] B.P. Abbott et al. (LIGO Scientific Collaboration and Virgo Collaboration), *Observation of Gravitational Waves from a Binary Black Hole Merger*, Phys. Rev. Lett. 116, 061102

[6] LIGO Caltech, Gallery, URL: https://www.ligo.caltech.edu/image/ligo20160615f (12.04.2021.)

[7] Romano, J. D. *Searches for stochastic gravitational-wave backgrounds*, Les Houches Summer School (July 2018)

[8] European Space Agency, URL: https://www.cosmos.esa.int/documents/387566/425793/2015_SMICA_CMB/ (25.03.2021.)

[9] Dicke, R. H., Peebles, P. J. E., Roll, P. G. and Wilkinson, D.T., *Cosmic Black-Body Radiation*, ApJ, 142, 414-419 (July 1965)

[10] Penzias, A. A. and Wilson, R. W., *A Measurement of Excess Antenna Temperature at 4080 Mc/s.*, ApJ, 142, 419–421 (July 1965)

[11] European Space Agency, Planck and the cosmic microwave background, URL: https://www.esa.int/Science_Exploration/Space_Science/Planck/Planck_and_the_cosmic_microwave_background (25.03.2021.)

[12] Allen, B., *The Stochastic Gravity-Wave Background: Sources and Detection*, Marck, J.-A. and Lasota, J.-P., eds., Relativistic Gravitation and Gravitational Radiation, p. 373, (1997).

[13] Jaranowski, P. and Krolak, A., *Analysis of Gravitational-Wave Data*, Cambridge University Press, New York 2009.

[14] Mazumdar, A. and White, G., *Review of cosmic phase transitions: their significance and experimental signatures*, Rep. Prog. Phys. 82 076901 (2019)

[15] Seljak, U. and Zaldarriaga, M., *Signature of gravity waves in polarization of the microwave background*, Phys. Rev. Lett., 78, 2054-2057 (1997)

[16] Shapiro Key, J., *Characterizing astrophysical sources of gravitational waves*, Doctoral Thesis (2010)

[17] Giesler, M., Isi, M., Scheel, M. A. and Teukolsky, S. A., *Black Hole Ringdown: The Importance of Overtones*, Physical Review X 9, 041060 (2019)

[18] Moore, C. J., Cole, R. H. and Berry C. P. L., *Gravitational-wave sensitivity curves*, arXiv:1408.0740

[19] Desjacques, V., Jeong, D. and Schmidt, F., *Large-Scale Galaxy Bias*, arXiv:1611.09787v5

[20] Springel, V., Frenk C. S. and White, S. D. M., *The large-scale structure of the Universe*, Nature (London)440, 1137 (2006), arXiv:astro-ph/0604561

[21] Fujita, T. and Vlah, Z., *Perturbative description of biased tracers using consistency relations of LSS*, arXiv:2003.10114v2

[22] McDonald, P. and Roy, A., *Clustering of dark matter tracers: generalizing bias for the coming era of precision LSS*, arXiv:0902.0991v1

[23] Wikipedia, Matter power spectrum, URL: https://en.wikipedia.org/wiki/Matter_power_spectrum (05.06.2021.)

[24] ESA and the Planck Collaboration, URL: https://www.cosmos.esa.int/documents/387566/1753103/ Planck_2018_pk_compilation.pdf (05.06.2021.)

[25] NASA, Goddard Space Fight Center, Tools, CAMB, URL: https://lambda.gsfc.nasa.gov/toolbox/tb_camb_form.cfm (25.06.2021.)

[26] Planck collaboration, *Planck 2018 results. VI. Cosmological parameters*, arXiv:1807.06209